

Impact of Defects on the Surface Chemistry of ZnO(000 $\bar{1}$)–O

Robert Lindsay,^{*,†} Ela Michelangeli,[†] Benjamin G. Daniels,[†] Timothy V. Ashworth,[†]
Adam J. Limb,[†] Geoffrey Thornton,[†] Aurora Gutiérrez-Sosa,[‡] Alessandro Baraldi,[§]
Rosanna Larciprete,^{||} and Silvano Lizzit^{||}

*Contribution from the Surface Science Research Centre and Chemistry Department,
Manchester University, Manchester M13 9PL, U.K., Physics Department, UMIST, P.O. Box 88,
Manchester M60 1QD, U.K., Dipartimento di Fisica, Via Valerio 2, 34127 Trieste and
Laboratorio TASC-INFN, S.S. 14 Km 163.5 Basovizza, 34012 Trieste, Italy, and
Sincrotrone Trieste S.C.p.A., S.S. 14 Km 163.5, 34012 Trieste, Italy*

Received February 12, 2002

Abstract: Scanning tunneling microscopy and core level photoelectron spectroscopy measurements have been used to investigate the morphology of ZnO(000 $\bar{1}$)–O, and its reactivity with carbon monoxide and carbon dioxide, as a function of surface preparation. Real space images of the surface indicate that increasing the substrate anneal temperature during preparation significantly reduces the surface step density. Surface defect concentration is also monitored by employing formic acid as a chemical probe, which is shown to adsorb dissociatively ($\text{HCOOH} \rightarrow [\text{HCOO}]^- + \text{H}^+$) only on zinc cations at step edges. Carbon 1s X-ray photoelectron spectra show that carbon monoxide and carbon dioxide both react to form surface carbonate species. Spectra, recorded both as a function of surface preparation and following coadsorption, demonstrate that the carbonate formed from either reactant molecule is located at oxygen vacancies at step edges, evidencing the significant role that defects can play in the surface chemistry of ZnO(000 $\bar{1}$)–O.

1. Introduction

Defects (e.g., vacancies, adatoms, and steps) at metal oxide surfaces are thought to significantly influence a variety of surface properties, including chemical reactivity. For example, it has recently been concluded that the dissociation of H_2O molecules on $\text{TiO}_2(110)1 \times 1$, at low temperature and pressure, requires the presence of surface oxygen vacancies.¹ However, there is a paucity of other studies that have examined the role of defects in the surface chemistry of metal oxides. This lack of experimental data needs to be addressed, as various commercially important applications of metal oxides depend on the chemistry occurring at their surfaces, for example, heterogeneous catalysis, corrosion inhibition, and gas sensing. In this study, we contribute to this challenging area, demonstrating that surface defects are pivotal to the surface chemistry of carbon monoxide (CO) and carbon dioxide (CO_2) on ZnO(000 $\bar{1}$)–O. To do so, we employ X-ray photoelectron spectroscopy (XPS), together with scanning tunneling microscopy (STM).

Briefly, bulk terminated ZnO(000 $\bar{1}$)–O is composed of a topmost layer of nearly-close packed oxygen anions, located at a short vertical distance (0.613 Å) above a second layer of Zn cations. Schematics of this polar surface are illustrated in Figure

1. Following the ionic model of bonding, such a polar surface is expected to be unstable.² Recent surface X-ray diffraction (SXRD) studies, however, have determined that the only significant shift away from bulk termination is an inward relaxation of the surface layer oxygen anions.^{3,4} One possible explanation for this seemingly contradictory result is that the near ideal surface structure is stabilized through surface-enhanced covalency, as indicated by ab initio calculations.⁴

An additional aspect of the surface geometric structure, revealed by STM, is that defect density, in the form of steps which have $\{10\bar{1}0\}$ oriented faces, can be quite significant.⁵ Surface defects have also been evidenced by the presence of adsorbed formate ($[\text{HCOO}]^-$), following exposure to formic acid (HCOOH).^{6–9} This deduction is made on the basis that on the ideal ZnO(000 $\bar{1}$)–O surface, there are no undercoordinated surface Zn cations to which a formate anion can bond. Zn cations in the second layer are fully coordinated (four) and are largely obstructed by the surface oxygen anions. Thus, surface formate indicates that there are available zinc ions at the surface,

* To whom correspondence should be addressed. E-mail: ryl@ssci.liv.ac.uk.

[†] Manchester University.

[‡] UMIST.

[§] Laboratorio TASC-INFN.

^{||} Sincrotrone Trieste S.C.p.A.

(1) Brookes, I. M.; Murny, C. A.; Thornton, G. *Phys. Rev. Lett.* **2001**, *87*, 266103.

(2) Tasker, P. W. *J. Phys. C: Solid State Phys.* **1979**, *12*, 4977.

(3) Jedrecy, N.; Sauvage-Simkin, M.; Pinchaux, R. *Appl. Surf. Sci.* **2000**, *162/163*, 69.

(4) Wander, A.; Schedin, F.; Steadman, P.; Norris, A.; McGrath, R.; Turner, T. S.; Thornton, G.; Harrison, N. M. *Phys. Rev. Lett.* **2001**, *86*, 3811.

(5) Parker, T. M.; Condon, N. G.; Lindsay, R.; Leible, F. M.; Thornton, G. *Surf. Sci.* **1998**, *415*, L1046.

(6) Vohs, J. M.; Barteau, M. A. *J. Catal.* **1988**, *113*, 497.

(7) Ludviksson, A.; Zhang, R.; Campbell, C. T.; Griffiths, K. *Surf. Sci.* **1994**, *313*, 64.

(8) Barteau, M. A. *Chem. Rev.* **1996**, *96*, 1413.

(9) Gutierrez-Sosa, A.; Evans, T. M.; Woodhead, A. P.; Lindsay, R.; Murny, C. A.; Thornton, G.; Yoshihara, J.; Parker, S. C.; Campbell, C. T.; Oldman, R. J. *Surf. Sci.* **2001**, *477*, 1.

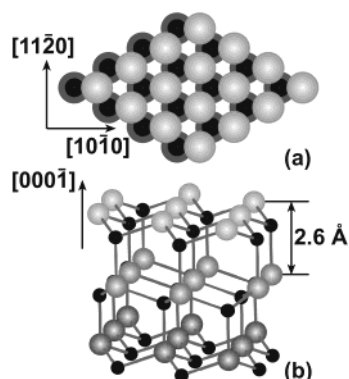


Figure 1. (a) Space filling model of plan view of ZnO(000 $\bar{1}$)–O surface. (b) Ball and stick model of ZnO, oriented such that the ZnO(000 $\bar{1}$)–O surface is at the top. The indicated distance (2.6 Å) is that of a single double-layer step height. In both diagrams, larger (smaller) spheres are oxygen (zinc) ions.

which must be because of one or more types of defect. We note that the {10 $\bar{1}$ 0} oriented steps, apparent in STM,⁵ expose Zn cations.

Studies focusing on the surface chemistry of ZnO(000 $\bar{1}$)–O are largely motivated by the emergence of ZnO as a model catalyst support, arising from its use in methanol synthesis, and also fundamental interest in the reactivity of polar surfaces, in general. Previous work has included a number of investigations of the adsorption of CO and CO₂,^{10–19} both of which are components of the methanol synthesis feedstock. However, the results of these studies, outlined below, are apparently somewhat divergent.

Au et al. employed a combination of core level and valence band photoelectron spectroscopy to probe the interaction of CO and CO₂ with ZnO(000 $\bar{1}$)–O.¹⁰ For CO, they evidenced adsorption on an oxygen annealed *defect-free* surface, but not, within the sensitivity limits of their measurements, on a sputtered surface (*defect-enriched*). More specifically, after exposure of the surface at 120 K to 100 L of CO, the principal surface species was concluded to be molecular CO, along with a small amount of carbonate (CO₃²⁻). Extended CO exposure (10⁴ L) at the same substrate temperature led to a significant increase in CO₃²⁻ concentration, the appearance of physisorbed CO₂, and the complete loss of surface CO. Annealing this surface to 300 K left only CO₃²⁻ on the surface. CO₂ adsorption at 100 K also gave rise to surface CO₃²⁻, but in sharp contrast to CO, the adsorption was much more pronounced on the *defect-enriched* surface. In this case, the only other surface species observed was physisorbed CO₂, which desorbed at substrate temperatures of between 100 and 145 K.

More recent C K-edge NEXAFS data^{11,12} confirm Au et al.'s conclusion¹⁰ that CO₃²⁻ is formed on ZnO(000 $\bar{1}$)–O, following exposure to either CO or CO₂ at low temperature (130 K). Additionally, the polarization dependence of the NEXAFS spectra indicates that the angular geometry of CO₃²⁻ resulting from either CO or CO₂ adsorption is very similar, the molecular plane tilting approximately 30° away from the surface normal. There is, however, a striking difference between the NEXAFS study and Au et al.'s results, in that although the NEXAFS measurements were all recorded from a supposedly *defect-free* surface, a similar concentration of surface CO₃²⁻ (0.1 ± 0.05 ML) was obtained from both CO and CO₂ adsorption.

CO adsorption on ZnO(000 $\bar{1}$)–O has also been the subject of several other studies. In contrast to the work described above, temperature-programmed desorption (TPD) and Fourier transform reflection–absorption infrared spectroscopy (FT-RAIRS) data show no indication of CO adsorption at 130 K.^{11,13} We note that for both of these measurements, the lack of adsorbate signal has previously been concluded to be probably a consequence of a lack of experimental sensitivity.¹² Adsorption is evidenced in the temperature range 77–180 K in investigations conducted by Becker et al., but the only surface species is concluded to be molecular CO.^{14–16} Valence band photoemission spectra recorded at a substrate temperature of 80 K in high ambient pressures of CO were also interpreted as indicating that the resulting adsorbed moiety is CO.^{17–19}

From the preceding discussion it is clear that, to date, there are significant discrepancies in the results of studies of CO and CO₂ adsorption on ZnO(000 $\bar{1}$)–O. One possible origin of these anomalies is variation in surface structure, explicitly the density of surface defects, arising from differences in substrate preparation. To test this hypothesis, we have employed STM to probe surface structure as a function of surface preparation, and XPS to examine the reactivity of variously prepared surfaces toward CO and CO₂. Additionally, formic acid is used as a chemical probe to measure the concentration of available zinc cations. Our results demonstrate a clear relationship between surface defect density and reactivity.

2. Experimental Section

STM images were acquired using an Omicron variable temperature ultrahigh vacuum (UHV) STM. Data were recorded in the constant current mode, with the sample biased positively with respect to the tip. Sample biases of 3.5 and 4.2 V, and a tunneling current of 0.5 nA, were used to obtain the images depicted in Figure 2. A variety of other tunneling parameters were tested, but none led to improved image quality. The substrate temperatures during data acquisition were ~293 and ~237 K in Figure 2a and b, respectively. We note that on the basis of other slightly less well-resolved images, there is no evidence to suggest that such a change in temperature (~56K) altered the observed sample morphology.

XPS data were recorded in two separate UHV chambers, employing Al K α X-rays ($h\nu = 1486.6$ eV) and synchrotron radiation as photon sources, respectively. For the line source (TA10, VSW), photoelectrons were analyzed using a VSW/Omicron EA125 electron energy analyzer with a five-channeltron detection system. Data were collected with an analyzer pass energy of 20 eV and the analyzer lens in high-magnification mode, resulting in an energy resolution of $\Delta E = 1$ eV (full width at half maximum (fwhm)) and an angular acceptance of $\Delta\theta = \pm 8^\circ$ (fwhm) for all of the measurements. The angle subtended by the X-ray source and entrance lens of the analyzer, which lay in the horizontal plane, was 70° in plane, and 45° out of plane. A photoelectron emission angle of 23° was used for the data presented in this paper.

- (10) Au, C. T.; Hirsch, W.; Hirschwald, W. *Surf. Sci.* **1988**, *197*, 391.
 (11) Gutiérrez-Sosa, A.; Crook, S.; Haq, S.; Lindsay, R.; Ludviksson, A.; Parker, S.; Campbell, C. T.; Thornton, G. *Faraday Discuss.* **1996**, *105*, 355.
 (12) Lindsay, R.; Gutiérrez-Sosa, A.; Thornton, G.; Ludviksson, A.; Parker, S.; Campbell, C. T. *Surf. Sci.* **1999**, *439*, 131.
 (13) Ludviksson, A.; Ernst, K. H.; Zhang, R.; Campbell, C. T. *J. Catal.* **1993**, *141*, 380.
 (14) Becker, Th.; Boas, Ch.; Burghaus, U.; Wöll, Ch. *Phys. Rev. B* **2000**, *61*, 4538.
 (15) Becker, Th.; Boas, Ch.; Burghaus, U.; Wöll, Ch. *J. Vac. Sci. Technol., A* **2000**, *18*, 1089.
 (16) Becker, Th.; Kunat, M.; Boas, Ch.; Burghaus, U.; Wöll, Ch. *J. Chem. Phys.* **2000**, *113*, 6334.
 (17) Gay, R. R.; Nodine, M. H.; Henrich, V. E.; Zeiger, H. J.; Solomon, E. I. *J. Am. Chem. Soc.* **1980**, *102*, 6752.
 (18) D'Amico, K. L.; Trenary, M.; Shinn, N. D.; Solomon, E. I.; McFeely, F. R. *J. Am. Chem. Soc.* **1982**, *104*, 5102.
 (19) Didziulis, S. V.; Butcher, K. D.; Cohen, S. L.; Solomon, E. I. *J. Am. Chem. Soc.* **1989**, *111*, 7110.

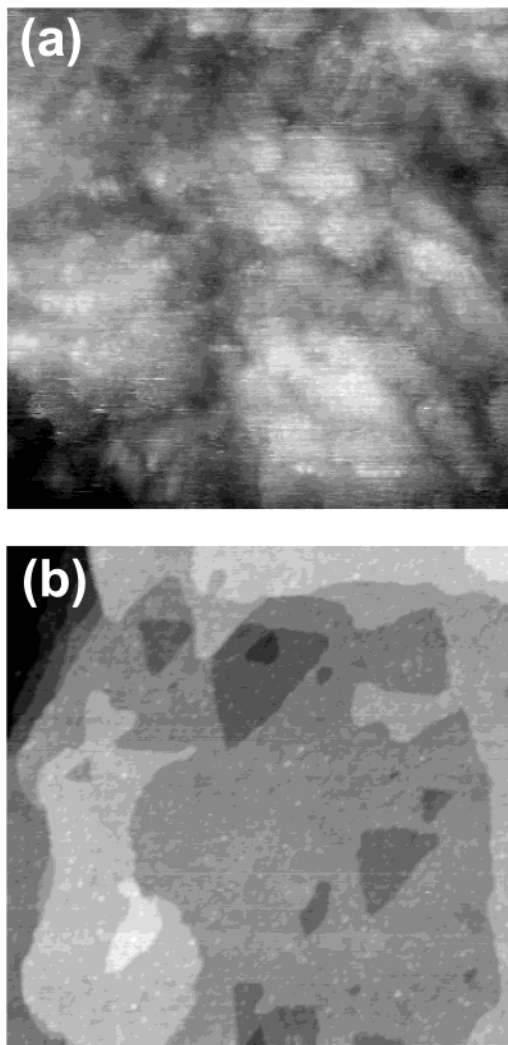


Figure 2. $1800 \times 1800 \text{ \AA}^2$ constant current mode STM images of ZnO(000 $\bar{1}$)-O, following annealing at 1020 (a) and 1500 K (b). The images were acquired at 293 and 237 K with sample biases of 3.5 and 4.2 V, for (a) and (b), respectively, and a tunneling current of 0.5 nA.

The synchrotron radiation XPS measurements, which will henceforth be referred to as *high resolution*, were performed at the SuperESCA beam line at the ELETTRA synchrotron radiation facility in Trieste, Italy.²⁰ A double pass electron energy analyzer, equipped with a 96 channel detection system, was used to collect the photoelectron spectra.²¹ An overall energy resolution of $\Delta E = 0.2 \text{ eV}$ (fwhm) was employed. The angle between the entrance lens of the analyzer and the incoming photon beam was 40° in the horizontal plane. Spectra were obtained at a photoelectron emission angle of 20° .

In situ preparation of the ZnO(000 $\bar{1}$)-O surface involved a basic prescription of repeated Ar⁺ bombardment (typical parameters employed were an accelerating potential of 500 V and a beam current on the order of several $\mu\text{A}/\text{cm}^2$ for periods of ~ 20 min at an angle of incidence between normal and 45°) and anneal cycles. Samples were subjected to a number of different maximum anneal temperatures (measured using an optical pyrometer), to investigate the variation of this parameter on surface structure and reactivity. Additionally, a final anneal at lower temperatures (870–570 K) in a partial pressure of oxygen (1×10^{-6} mbar) was sometimes performed, to examine the effect of this

procedure, which has been proposed as a means of restoring surface stoichiometry (by removing oxygen vacancies).²² For the two STM images displayed in Figure 2, the peak anneal temperatures were 1020 (90 min) and 1500 K (120 min). The synchrotron-based data were acquired from a surface annealed at 870 K (30 min). Five distinct surface preparations were performed for the Al K α XPS measurements: a maximum anneal temperature of 1070 K (300 min); a maximum anneal temperature of 1070 K (300 min) with final anneal in a partial pressure of oxygen (20 min); a maximum anneal temperature of 1220 K (300 min); a maximum anneal temperature of 1370 K (300 min); and a maximum anneal temperature of 1370 K (300 min) with final anneal in a partial pressure of oxygen (20 min). It should be noted that we have found that there can be a substantial difference (up to 100–200 K lower) between the measured and actual temperature of the oxide surface when annealing. Temperature increments, however, are significantly more reliable, at least within one set of measurements, which is the important factor for this work. For all of the preparations, surface order and cleanliness were monitored by low-energy electron diffraction (LEED), and either XPS or Auger electron spectroscopy (AES), respectively. All of the data presented in this paper were recorded from samples exhibiting 1×1 LEED patterns.

Exposure of the substrate to CO, CO₂, and HCOOH was achieved by simply back filling the UHV chambers up to a maximum of $\sim 2 \times 10^{-5}$ mbar. Prior to admitting the formic acid to a chamber, it was thoroughly degassed via repeated freeze–thaw cycles. Gas/vapor purity was confirmed with in situ mass spectrometers. Saturation adsorbate coverages were ensured by repeatedly dosing the substrate and recording photoelectron spectra. Exposures of up to 10^3 L for HCOOH and 10^4 L for CO and CO₂ were employed. Details of the sample temperatures during dosing and measurement are given below.

3. Results

Representative large-scale ($1800 \times 1800 \text{ \AA}^2$) STM images of ZnO(000 $\bar{1}$)-O following annealing at 1020 and 1500 K are shown in Figure 2a and b, respectively. A direct comparison of the two images evidences significant differences in surface morphology. In image a, the lower temperature (1020 K) annealed surface, no well-defined terraces or step edges are discernible; rather, the surface appears to be somewhat disordered and rough. This morphology is very similar to that reported by Bonnell's group, who have recorded STM data from a ZnO(000 $\bar{1}$)-O surface which had been annealed at approximately 970 K.^{23,24} In contrast, the structure of the 1500 K annealed surface (Figure 2b) is much more distinct, in that relatively large, flat terraces with sharp step edges are observed. The measured step heights match those expected for either single (2.6 \AA) or multiple double-layer steps (see Figure 1b). This image resembles STM data from ZnO(000 $\bar{1}$)-O presented in ref 5, which was recorded at room temperature, including the presence of triangular pit features, which are rotated on alternate terraces. We note that performing a final anneal in a partial pressure of oxygen did not give rise to any apparent changes in surface structure on the length scale investigated with STM.

Three *high-resolution* C 1s XPS spectra ($h\nu = 425 \text{ eV}$), recorded from ZnO(000 $\bar{1}$)-O, are shown in Figure 3. Prior to data acquisition, the surface had been prepared by annealing at 870 K, and then dosed with either HCOOH (~ 3 L) at a substrate temperature of 293 K, or CO (~ 700 L) or CO₂ (~ 2 L) at 120 K. All of the spectra exhibit a single principal feature. *High-*

(20) Baraldi, A.; Barnaba, M.; Brena, B.; Cocco, D.; Comelli, G.; Lizzit, S.; Paolucci, G.; Rosei, R. *J. Electron Spectrosc. Relat. Phenom.* **1995**, *76*, 145.

(21) Baraldi, A.; Dhanak, V. R. *J. Electron Spectrosc. Relat. Phenom.* **1994**, *67*, 211.

(22) Ernst, K. H.; Ludviksson, A.; Zhang, R.; Yoshihara, J.; Campbell, C. T. *Phys. Rev. B* **1993**, *47*, 13782.

(23) Rohrer, G. S.; Bonnell, D. A. *Surf. Sci.* **1991**, *247*, L195.

(24) Thibado, P. M.; Rohrer, G. S.; Bonnell, D. A. *Surf. Sci.* **1994**, *318*, 379.

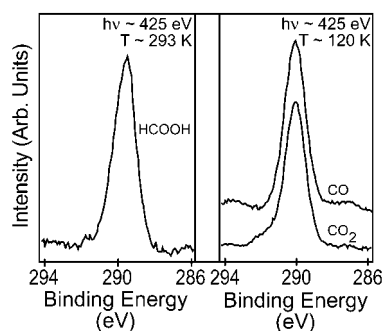


Figure 3. C 1s XPS spectra recorded from ZnO(0001)-O (870 K annealed surface), following exposure to HCOOH (~ 3 L) at a substrate temperature of 293 K (left panel), CO (~ 700 L) and CO₂ (~ 2 L) at 120 K (right panel). XPS measurements were performed at the dosing temperatures.

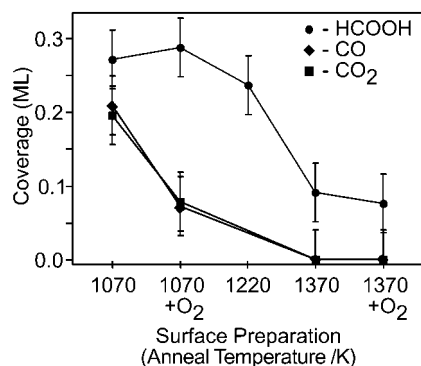


Figure 4. Plots of saturation coverage of [HCOO]⁻, resulting from exposure to HCOOH at ~ 310 K, and CO₃²⁻, resulting from exposure to either CO or CO₂ at ~ 120 K, versus ZnO(0001)-O surface preparation. Data were obtained at the same substrate temperature as the dosing was performed.

resolution C 1s XPS data were also recorded following both higher temperature anneals (1270 K) in a vacuum, and annealing in a partial pressure of oxygen. No other significant features were observed, except sometimes a small peak at approximately 285 eV binding energy (BE), which we assign to adsorbed atomic carbon⁹ (XPS BE's were calculated using the Fermi level, obtained from the metallic sample holder, and the Zn 3s peak, which is taken to be at 139.8 eV⁹).

For HCOOH exposure, the C 1s XPS peak is centered at a BE of 289.6 ± 0.3 eV. As expected from earlier work,⁹ this value is consistent with there only being [HCOO]⁻ adsorbed on the surface at room temperature (293 K); molecular HCOOH desorbs at around 180 K.⁷ The BE's of the principal peaks following CO and CO₂ dosing are, within experimental error, identical, that is, 290.0 ± 0.3 eV. By reference to Au et al.'s work,¹⁰ we attribute this result to surface CO₃²⁻ being formed from both CO and CO₂. Such an assignment is supported by C K-edge NEXAFS data,¹¹ which show conclusively that the adsorption of both CO and CO₂ leads to CO₃²⁻ on ZnO-(0001)-O. The small shoulder in the spectrum of the CO₂ dosed surface, at approximately 292 eV BE, is, on the basis of ref 10, most probably because of the presence of a small amount of physisorbed CO₂. Unlike earlier studies,¹⁰⁻¹² no other surface species are observed following CO adsorption (e.g., molecular CO, BE = 288.6 eV¹⁰). This disparity is most likely simply because of the fact that in the present studies the actual surface temperature is somewhat greater than that in the earlier work.

Figure 4 displays, as a function of surface preparation, the [HCOO]⁻ and CO₃²⁻ saturation coverages obtained following

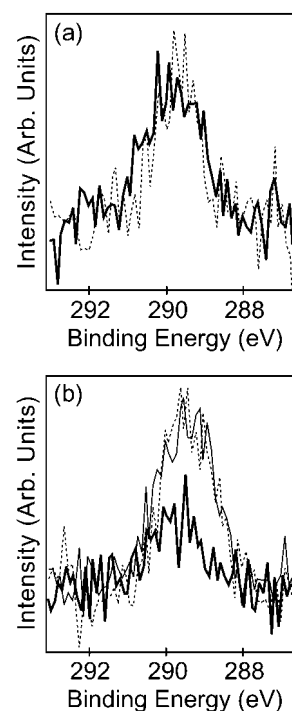


Figure 5. C 1s XPS spectra ($h\nu = 1486.6$ eV) recorded from ZnO-(0001)-O (1070 K annealed surface) showing results of coadsorption measurements. The surface was exposed to the following gas/vapor prior to data acquisition: (a) CO₂ (broken line), CO₂ plus CO (solid line); (b) CO₂ (bold line), CO₂ plus HCOOH (thin line), HCOOH (broken line).

exposure to HCOOH (●) at a substrate temperature of ~ 310 K, CO (◆) and CO₂ (■) at ~ 120 K. Coverage calculations were based upon standard analysis methods²⁵ and calculated photoionization cross sections,²⁶ utilizing C 1s and Zn 3s core level peaks acquired with Al K α photons. One monolayer (ML) is defined here as one adsorbate molecule per surface layer oxygen atom. The error bars for coverage in Figure 4 have been estimated from the signal-to-noise ratio of the Al K α XPS spectra (see Figure 5 for examples of such data). It should be pointed out that for these XPS measurements, the substrate was sputtered with high-energy argon ions (3 keV) for 1 h to create a thoroughly disordered surface prior to preparing a different temperature annealed surface. This was carried out to rule out the possibility that previous preparations could influence later results. The utility of this method is demonstrated by the observation that the reactivity of the surface, as measured by extent of [HCOO]⁻ uptake, could be returned from the 1370 K annealed surface to the 1070 K annealed surface by this procedure.

All three plots in Figure 4 indicate that increasing the anneal temperature during surface preparation leads to lower adsorbate coverage. For [HCOO]⁻, the coverage decreases from 0.27 ± 0.04 ML at a substrate anneal temperature of 1070 K to 0.09 ± 0.04 ML at 1370 K. Within the experimental uncertainty, a final anneal in a partial pressure of oxygen does not change the saturation coverage of [HCOO]⁻. The two CO₃²⁻ coverage data sets are almost identical to each other. As well as the decrease in coverage from approximately 0.2 ML to zero (the lower limit of detection is estimated to be about 0.05 ML) with anneal

(25) *Practical Surface Analysis*, 2nd ed.; Briggs, D., Seah, M. P., Eds; Wiley: Chichester, 1990; Vol. 1.

(26) Yeh, J. J.; Lindau, I. *At. Data Nucl. Data Tables* **1985**, 32, 1.

temperature, there is also, in contrast to $[\text{HCOO}]^-$, a significant decrease in coverage because of annealing in oxygen, as indicated by the 1070 and 1070 K + O₂ data points.

All K α XPS spectra were also recorded following coadsorption of (i) CO₂ and CO, and (ii) CO₂ or CO, and HCOOH. In Figure 5a, C 1s spectra of ZnO(000 $\bar{1}$)–O, prepared by annealing at 1070 K, initially saturated with CO₂ (broken line), and then subsequently dosed with 10⁴ L of CO (solid line) at 120 K, are depicted. There is no apparent change in C 1s intensity, indicating that there is no increase in CO₃²⁻ concentration on the coadsorbed surface. Spectra from a similar surface dosed with CO₂ (bold line), but then subsequently exposed to a saturation dose of HCOOH (500 L) at room temperature (thin line), are illustrated in Figure 5b. In this case, the coadsorbed surface exhibits an increase in C 1s intensity. Comparison of this coadsorption spectrum with one obtained from an analogously prepared surface saturated with HCOOH alone (broken line in Figure 5b) demonstrates that the coverage of carbon-containing species for these two differently dosed surfaces is, within experimental error, the same.

4. Discussion

From the above measurements, it is apparent that surface preparation influences both the surface structure and the reactivity of ZnO(000 $\bar{1}$)–O. The STM images, displayed in Figure 2, clearly demonstrate that increasing the substrate anneal temperature (1020–1500 K) during preparation leads to a much flatter surface morphology, with larger terrace sizes and lower step density. Thus, it may be concluded that defect density, in the form of steps, can be controlled by varying the substrate anneal temperature. A high step density at lower substrate anneal temperatures is consistent with earlier He-atom scattering^{14,16} and SXRD³ data, which indicate the presence of small, sub 100 Å, average terrace widths, after relatively low anneal temperatures of 850 and 1073 K, respectively. Lower dimensional defects, such as oxygen vacancies, could not be investigated by STM, because of the lack of atomic scale resolution in this study. It should be noted that previous work²⁷ indicates that at the anneal temperatures we employed, in particular, the higher maximum temperatures, some of the substrate material (ZnO) would, almost certainly, have been desorbed during an annealing cycle. We tentatively suggest that such desorption may aid the formation of flatter surface morphologies.

Defects are also evidenced, chemically, by the uptake of finite amounts of $[\text{HCOO}]^-$, which only adsorbs at available undercoordinated zinc cations on ZnO(000 $\bar{1}$)–O.^{6–9} On the basis of the STM results, the decrease in $[\text{HCOO}]^-$ saturation coverage with increasing anneal temperature (Figure 4) is consistent with at least a significant proportion of the surface $[\text{HCOO}]^-$ being located at steps. Inclusion of oxygen annealing in surface preparation, which is undertaken in an attempt to reduce surface oxygen vacancy density,²² has no effect on the coverage of $[\text{HCOO}]^-$. From this observation, it may be proposed that either oxygen annealing does not deplete oxygen vacancies or the adsorption of $[\text{HCOO}]^-$ does not depend on the existence of such defects. Given that oxygen annealing does decrease the concentration of surface CO₃²⁻ (Figure 4), we deduce that the latter of these two possibilities is correct. Thus, we can conclude that $[\text{HCOO}]^-$ does not adsorb on undercoordinated Zn cations

at oxygen vacancy sites, but rather only on the Zn cations exposed at step edges.⁵ Hence, the concentration of surface $[\text{HCOO}]^-$ probes step density, rather than the total concentration of undercoordinated Zn cations.

As for surface CO₃²⁻ formation from CO and CO₂, the very similar behavior in saturation coverage versus sample preparation (Figure 4) for the two reactants suggests a degree of similarity in their reaction pathways, even though CO₂ requires one substrate oxygen to form CO₃²⁻, whereas two are necessary for CO. This proposition is supported by the absence of a change in surface coverage in the CO₂/CO coadsorption experiment (Figure 5a), which demonstrates that the CO₃²⁻ adsorption site is the same for both CO and CO₂. Previous NEXAFS data are also indicative of an identical surface location, in that similar angular geometries for CO₃²⁻ are determined following either CO or CO₂ exposure.^{11,12}

Concerning changes in saturation coverage with surface preparation, CO₃²⁻, analogous to $[\text{HCOO}]^-$, decreases with increasing anneal temperature, but, unlike $[\text{HCOO}]^-$, there is also a reduction after oxygen annealing. Following the reasoning above for $[\text{HCOO}]^-$, these data indicate that both steps and oxygen vacancies are involved in the generation of surface CO₃²⁻. Two possible simple scenarios arise from this conclusion: either oxygen vacancies and steps act as independent adsorption sites for CO₃²⁻, or CO₃²⁻ is located at an oxygen vacancy at a step edge. The second option is favored by the fact that for any specific surface preparation, the CO₃²⁻ coverage is always lower than $[\text{HCOO}]^-$, suggesting a smaller number of adsorption sites for CO₃²⁻, and is confirmed by the CO₂/HCOOH coadsorption measurements depicted in Figure 5b. These data show that CO₃²⁻ occupies a subset (oxygen vacancies at steps) of the $[\text{HCOO}]^-$ adsorption sites (steps), because exposing a CO₃²⁻ covered surface to HCOOH leads to the same total adsorbate coverage as a surface saturated with $[\text{HCOO}]^-$ alone. If CO₃²⁻ was also located in oxygen vacancies away from steps, then the CO₂/HCOOH coadsorption coverage would be greater than that following only HCOOH exposure. One obvious question arising from our proposed location of CO₃²⁻ is why the coverage of CO₃²⁻ does not go to zero for the 1070 K surface annealed in oxygen. The answer is simply that the oxygen vacancies are not completely removed by annealing in a partial pressure of oxygen, but are rather significantly depleted.

Besides demonstrating the importance of defects in the chemistry of CO and CO₂ on ZnO(000 $\bar{1}$)–O, the results presented here are also valuable in regards to other studies of this surface. The STM data directly demonstrate that significantly higher anneal temperatures than those typically employed (e.g., 850 K^{14–16}) for surface preparation are needed to form surfaces with low step densities. We suggest that this requirement may also extend to other ZnO surfaces (e.g., ZnO(0001)–Zn). Additionally, the role of defects must be considered to further understand the interaction of other adsorbates with this surface. For example, it has been found that CO dosed onto a ZnO(000 $\bar{1}$)–O surface covered with 0.5 ML of Cu in the form of 2-D islands is adsorbed as molecular CO.^{11–13} Given that we have concluded that CO₃²⁻ is formed at oxygen vacancies at step edges, it follows that Cu almost certainly initially decorates such sites. This interpretation is consistent with data suggesting that Cu first adsorbs at defects on this surface.²⁸ A

(27) Göpel, W.; Lampe, U. *Phys. Rev. B* **1980**, *22*, 6447.

(28) Thornton, G.; Crook, S.; Chang, Z. *Surf. Sci.* **1998**, *415*, 122.

further point concerning metal deposition is that through varying the surface preparation conditions and thus controlling defect concentration, it may be possible to modify the growth mode of Cu and other metals on ZnO(000 $\bar{1}$)–O.

5. Conclusions

STM images of ZnO(000 $\bar{1}$)–O indicate that increasing the substrate anneal temperature during preparation leads to flatter surfaces, and thus lower step densities. This trend is supported by XPS measurements of [HCOO][–] coverage, which we have found only adsorbs on available Zn cations at step edges. Photoelectron spectra recorded following exposure of ZnO(000 $\bar{1}$)–O to either CO or CO₂ indicate that the coverage of the resulting CO₃^{2–} species decreases for surface preparations

involving either a higher anneal temperature or a final anneal in a partial pressure of oxygen. Coadsorption of (i) CO₂ and CO, and (ii) CO₂ and HCOOH indicate, respectively, that the location of CO₃^{2–} on the surface is independent of reactant (i.e., CO or CO₂) and that it resides in a subset of the [HCOO][–] adsorption sites. Our interpretation of these various data is that they demonstrate that the formation of CO₃^{2–} from CO and CO₂ on ZnO(000 $\bar{1}$)–O is driven by the presence of surface defects, specifically oxygen vacancies at steps.

Acknowledgment. We thank ELETTRA, the European Union (EU contract no. HPRI-CT-1999-00033) and the EPSRC (U.K.) for supporting this work.

JA025904U